



Published in final edited form as:

Cardiovasc Eng Technol. 2015 September ; 6(3): 303–313. doi:10.1007/s13239-015-0221-2.

The consequence of biologic graft processing on blood interface biocompatibility and mechanics

Aurore B. Van de Walle, Joseph S. Uzarski, and Peter S. McFetridge

J. Crayton Pruitt Family Department of Biomedical Engineering, University of Florida, PO Box 116131, 1275 Center Drive, Gainesville, FL 32611

Abstract

Processing *ex vivo* derived tissues to reduce immunogenicity is an effective approach to create biologically complex materials for vascular reconstruction. Due to the sensitivity of small diameter vascular grafts to occlusive events, the effect of graft processing on critical parameters for graft patency, such as peripheral cell adhesion and wall mechanics, requires detailed analysis.

Isolated human umbilical vein sections were used as model allogenic vascular scaffolds that were processed with either: 1. sodium dodecyl sulfate (SDS), 2. ethanol/acetone (EtAc), or 3. glutaraldehyde (Glu). Changes in material mechanics were assessed via uniaxial tensile testing. Peripheral cell adhesion to the opaque grafting material was evaluated using an innovative flow chamber that allows direct observation of the blood-graft interface under physiological shear conditions.

All treatments modified the grafts tensile strain and stiffness properties, with physiological modulus values decreasing from Glu 240 ± 12 kPa to SDS 210 ± 6 kPa and EtAc 140 ± 3 kPa, $P < .001$. Relative to glutaraldehyde treatments, neutrophil adhesion to the decellularized grafts increased, with no statistical difference observed between SDS or EtAc treatments. Early platelet adhesion (% surface coverage) showed no statistical difference between the three treatments; however, quantification of platelet aggregates was significantly higher on SDS scaffolds compared to EtAc or Glu.

Tissue processing strategies applied to the umbilical vein scaffold were shown to modify structural mechanics and cell adhesion properties, with the EtAc treatment reducing thrombotic events relative to SDS treated samples. This approach allows time and cost effective prescreening of clinically relevant grafting materials to assess initial cell reactivity.

*Corresponding Author, TEL: (352) 273-9325, FAX: (352) 273-9221, pmcfetridge@bme.ufl.edu.

DISCLOSURE

The authors have no competing interest to declare.

No animal studies were carried out by the authors for this article.

All procedures followed were in accordance with the ethical standards of the responsible committee on human experimentation (institutional and national) and with the Helsinki Declaration of 1975, as revised in 2000 (5). Informed consent was obtained from all patients for being included in the study.

Keywords

biocompatibility; biomaterial; decellularization; flow chamber; human umbilical vein; vascular tissue engineering; thrombosis

INTRODUCTION

While autologous vessels are the grafts of choice for small diameter vascular bypass[1–3], they are severely limited in availability due to disease or prior use. Allogeneic grafts such as human umbilical veins (HUV) have been shown to be a viable clinical alternative in peripheral applications when crosslinked with aldehydes[4, 5]. The treatment of collagenous grafts with glutaraldehyde induces the modification of amino groups to allow the formation of covalent bonds, more specifically it crosslinks the lysyl amino acid residues of adjacent collagen monomers[6, 7]. This chemical reaction creates a barrier that limits the patient's immune and regenerative capacity, thus limiting remodeling and preventing functional recovery[8, 9]. While suitable for adult patients, the inability to remodel makes cross-linked materials unattractive for pediatric patients where vessel structure is continuously remodeled during growth. The inability to remodel into a competent tissue is also a primary limitation toward achieving fully functional vascular grafts that hypothetically improves outcomes. As such, considerable research effort has moved toward synthetic[10] or naturally derived[11–13] materials that are hydrolysable or enzymatically degradable to allow natural remodeling processes. This class of materials can be used as templates for guided regeneration or tissue engineering[14] with the aim of creating 'living' functional vessels. Herein, emphasis has been placed on *ex-vivo* derived vascular scaffolds for their biochemical composition and 3D microarchitecture that is preserved upon decellularization treatments.

The objective of tissue processing, or decellularization, is to remove soluble extracellular matrix (ECM) components and cells that would otherwise elicit negative immune responses and potentially lead to graft failure. This process strips away the existing endothelium exposing the underlying type IV collagen-rich basement membrane which is prone to thrombotic events[15, 16]. A variety of strategies to limit thrombogenicity have been explored including re-endothelialization of the graft lumen prior to implantation[17]; however, recent history has shown limited success as endothelial cells are often lost during surgical intervention or shear reperfusion[18–23]. Therefore, as part of a developmental strategy, it is critical to define the effect of chemical treatments on the grafts surface reactivity. Different treatments used to decellularize tissues are known to alter materials surface chemistry[24] and as such may significantly alter peripheral cell adhesion. Sodium dodecyl sulfate (SDS) and ethanol/acetone are used herein as representative examples of processing chemistries. SDS is an anionic surfactant that removes cellular material by solubilizing lipid membranes and nuclear remnants as well as stripping soluble glycosaminoglycans[25], growth factors, and insoluble macromolecules from the ECM[26]. By comparison, ethanol lyses cells via dehydration, and a mixture of ethanol and acetone (EtAc) is effective for extraction of lipids[27], but tends to crosslink the ECM proteins[28]. Evaluating acellular materials is critical in vascular applications but has proven problematic

due to difficulty evaluating complex surface chemistries and limited model systems to predict peripheral cell interactions.

Shear stress induced by blood flow is a recognized regulator of peripheral cell adhesion[29, 30], with parallel plate flow chambers having been used widely to mimic hemodynamic blood flow conditions and assess cell adhesion[31, 32]. However, these flow chambers are designed to study cell interactions with specific proteins coated on glass and as such these surfaces do not represent the complexity of natural tissues. In the present investigations, a novel flow chamber was designed and built using parallel plate flow geometry to expose the lumen of a vessel to peripheral blood cells under controlled shear conditions[33]. This flow chamber was used to assess the effects of tissue processing chemistries on the initial hemocompatibility of a model vascular scaffold derived from the human umbilical vein (HUV)[14, 15]. By comparing tissue decellularization methods to glutaraldehyde treatments (that have been used in the clinic for the past decades[4]) we aim to improve our understanding of how processing affects graft biocompatibility with the ultimate goal of generating an enhanced prosthesis.

MATERIALS AND METHODS

HUV isolation

Human umbilical veins (HUV) were extracted from umbilical cords freshly collected from UF Health Shands Hospital (Gainesville FL) (IRB approval #64–2010). Veins were isolated from the surrounding tissues to a uniform wall thickness of 0.75 mm using an automated dissection procedure then cut to 100 mm long segments, as previously described[12].

HUV processing treatments

Dissected veins were either decellularized (SDS or an ethanol acetone mixture (EtAc)), or cross-linked with glutaraldehyde (Glu). Decellularization was performed by immersing veins in either a solution of ethanol, acetone, and DI water (EtAc – 60:20:20 ratio), or 1% (w/v) sodium dodecyl sulfate (SDS) in DI water as previously described[15]. Briefly, samples were incubated in the decellularization solution under orbital shaking (100 RPM) conditions for 24 hours and rinsed in fresh aliquots of DI water. Sections were then incubated in deoxyribonuclease I (Sigma-Aldrich) (70 U/mL) at 37°C for 2 hours to remove nucleic acids, rinsed in DI water, and terminally sterilized in a solution of 0.2% peracetic acid and 4% ethanol in DI water. Scaffolds were then rinsed in DI water, and pH balanced (7.4) in PBS for 24 hours. Scaffolds were then stored in PBS at 4°C for a maximum of 2 weeks prior to use.

Cellular veins were crosslinked with 3% glutaraldehyde in PBS (Glu) for 1 hour under orbital shaking conditions (100 RPM)[5, 34]. Scaffolds were then rinsed in refreshed PBS solutions (pH 7.4) for 5, 15 and 40 minutes then 2 hours under constant agitation.

Tensile testing

Samples were cut into 5 mm wide ringlets and subjected to uniaxial tensile testing (Instron 5542, Norwood, Mass, using a 10N load cell). Tissue specimens (3 independent sample

groups from different cords, each assessed 5 times (15 discrete samples)) were preloaded to a stress of 0.01 N then elongated at a rate of 2 mm/min to determine physiological load values then at 5 mm/min until material failure. Mechanical properties were analyzed over the low-strain region that reflects physiologic behavior (physiologic range between 80–120 mmHg (11–16 kPa)). Stress/strain data was used to calculate the physiological tensile modulus (E) to determine the materials stiffness.

Blood draws

Human venous blood was harvested from healthy adult volunteers after obtaining informed consent (IRB approval #689–2010). Blood was collected in 10 U/mL of heparin using a 21-gauge needle and fluorescently labeled with 20 µg/mL of Acridine Orange (Molecular Probes).

Cell adhesion flow circuit design

Cell adhesion to the luminal surface of each differentially processed HUV sample was observed in real-time using the newly developed flow chamber designed to replicate earlier parallel plate geometries[33] (Figure 1 A&B). The chamber design allows the luminal surface of the HUV to be exposed to the flow channel. High-speed images were taken with a Zeiss AxioImager M2 upright epifluorescence microscope coupled with an AxioCam Hrm Rev 3 digital camera (Zeiss, Thornwood, NY) through a window located on the top plate of the flow chamber. Cell solutions were injected into the flow circuit prior to the chamber at controlled shear rates via a programmable syringe pump (PHD Ultra; Harvard Apparatus, Holliston, MA).

Neutrophil detachment assay

HL-60 promyelocytic leukemia cells transduced with a green fluorescent protein (GFP)-expressing lentiviral vector were generously provided by Dr. Christopher Cogle (University of Florida Department of Medicine, Gainesville, FL). Cells were maintained in Dulbecco's Modified Eagle Medium supplemented with 20% FBS and differentiated into neutrophils by incubation in 1.3% dimethylsulfoxide for 3 days as previously described[35]. Neutrophil-like differentiated HL-60 cells (dHL-60) were incubated with the HUV for 5h before applying a ramped flow (from 0.5 to 210 s⁻¹, flow was increased stepwise every 30 seconds) to assess their adhesion potential. The density of adherent dHL-60 neutrophils was quantified as shear values were ramped. At the initial (0.5 s⁻¹) and terminal (210 s⁻¹) shear rates dHL-60 density was assessed at 6 locations for each sample, (n=4), with assessments during shear ramping assessed at a single fixed location at 10x magnification to infer a larger count area (n=4).

Platelet adhesion assay

A longpass filter was used to detect acridine orange fluorescence (bound to platelet RNA). Validation of platelet staining was determined by adherent cells color, and size. Whole blood was perfused across the HUV surface at a calculated wall shear rate of 210 s⁻¹, and images were captured over a five minute perfusion period to assess dynamic aggregate formation. Fluorescent microscopy was performed using a Zeiss AxioImager M2 upright

fluorescence microscope with a Zeiss AxioCam Hrm Rev 3 digital camera operated by AxioVision software version 4.8. A threshold was applied to obtain a monochromatic mask of each image, with the percentage of white area corresponding to the percentage of platelet coverage and quantified at 60 second intervals. Platelet aggregates, referring to the accumulation of more than one platelet, were determined by size (diameter > 3 μm) and were manually counted using ImageJ (NCBI). An index indicative of the size of the aggregates for each treatment was calculated by dividing the percentage of platelet coverage by the number of aggregates for the seven discrete experiments over the 5 minutes of blood perfusion.

Histological analysis

Samples were embedded in Neg-50 media (Thermo Fisher Scientific, Waltham, MA) and snap-frozen in liquid nitrogen. Thin sections (7 μm) were cut and stained with hematoxylin and eosin using standard protocols and observed via the Zeiss AxioImager M2 upright microscope (Zeiss, Thornwood, NY).

SEM imaging

Samples were fixed in 2.5% glutaraldehyde, washed in PBS, fixed in 1% osmium tetroxide solution, and progressively dehydrated in 25%, 50%, 75%, 85%, 95%, and 3x100% ethanol solutions. Samples were then critical point dried, sputter coated with gold/palladium, and imaged using a Hitachi S-4000 FE-SEM at 10 kV.

Statistics

All values are presented as mean \pm standard errors of the mean. Significant differences between the means of more than one group were determined using one-way analysis of variance (ANOVA). If a significant difference ($P < 0.05$) was indicated by ANOVA, a Tukey post hoc test was used to compare between group means. Significant differences between two discrete groups were determined using the Student's *t*-test. *P* values < 0.05 indicate statistical significance in the mean values.

RESULTS

Effect of treatments on HUV architecture

Figure 2A shows morphological changes in the veins' structure immediately after each chemical treatment: EtAc treatments resulted in vessel contraction due to dehydration, while SDS veins expanded (Figure 2A). After rinsing and pH stabilization in PBS, SDS veins remained swollen, and EtAc veins rehydrated until reaching similar architecture as SDS treated samples. Glutaraldehyde treatments induced a characteristic color change (from light pink to yellow) and material stiffening. Unlike SDS scaffolds, EtAc scaffolds, and the vessels prior to treatment, Glu scaffolds maintained their tubular structure without luminal support upon pH balancing.

Scaffolds were further examined via histology coupled with SEM imaging to assess variation in fiber alignment and surface structure. Representative cross-sections stained with hematoxylin and eosin show cells and soluble components of the ECM remained present in

the native vein when compared to the acellular scaffolds (Figure 2B). Scanning electron micrographs show denudation of the endothelium by EtAc and SDS treatments showing the exposed subjacent basement membrane. Glu crosslinking processes resulted in a homogeneous ECM morphology on both lumen and ablumen surfaces. The effect was more evident on the abluminal surface where surface proteins appeared to have fused relative to SDS and EtAc treatments that were more fibrous in structure. Morphological observations also showed SDS treated scaffolds displayed partial disruption of the lumens basement membrane exposing the underlying ECM.

Material stiffness and tensile strain

Tensile analysis showed similar load/extension profiles for the three processing methods (Figure 3A inset). Within the physiological range, tensile modulus of the decellularized veins was lower than the Glu stabilized vessels (EtAc 140 ± 3 kPa, SDS 210 ± 6 kPa vs. Glu 240 ± 12 kPa; $P<.001$ and $P=.033$ respectively), with SDS treated grafts having significantly higher values than EtAc ($P<.001$) (Figure 3 A&B). With respect to the scaffold prior treatment, EtAc displayed a decreased tensile modulus ($P=.034$); Glu, an increased tensile modulus ($P=.004$); and SDS, no significant difference ($P>.05$). Additionally, tensile strain at 16 kPa (120 mmHg) was significantly higher for decellularized scaffolds compared to glutaraldehyde treatments (EtAc $21.2\pm 0.6\%$, SDS $19.2\pm 0.9\%$ vs. Glu $11.5\pm 0.9\%$; $P<.001$ for both) (Figure 3C). The tensile strain at 16 kPa was also significantly higher than the vessel prior to treatment for both decellularization approaches (EtAc: $P<.001$, SDS: $P=.047$), and was significantly lower for the glutaraldehyde treatment ($P=.006$).

Characterization of neutrophil dHL-60 adhesion

Neutrophil dHL-60 were seeded on each of the differentially processed HUV scaffolds and incubated for 5 hours, after which a low shear rate of 0.5 s^{-1} was applied to remove non-adherent cells and allow quantification of adhered neutrophils. Representative fluorescent images show significantly higher neutrophil dHL-60 adhesion to the decellularized grafts compared to glutaraldehyde stabilized grafts (EtAc 330 ± 62 cells/mm², SDS 314 ± 29 cells/mm² vs. Glu 98 ± 22 cells/mm²; $P=.001$ and $P=.002$ respectively) (Figure 4 A&B).

After ramping flow from below venous shear rates (0.5 s^{-1}) to arterial values (210 s^{-1}) the remaining adherent cells were quantified. Results showed a higher density for the decellularized groups compared to glutaraldehyde treated grafts (EtAc 235 ± 36 cells/mm², SDS 209 ± 161 cells/mm² vs. Glu 68 ± 30 cells/mm²; $P=.001$ and $P=.007$ respectively) (Figure 4B). Images taken during flow ramping show a progressive detachment of the dHL-60 neutrophils reaching detachment values of $40\pm 17\%$ (Glu), $46\pm 15\%$ (SDS), and $68\pm 6\%$ (EtAc) (Figure 4C).

Characterization of platelet adhesion

Direct observation of platelet/scaffold interactions shows single platelet adhesion to initiate aggregate formation within the first minute of blood perfusion (Figure 5A). SEM images taken after 5 minutes of perfusion confirm platelet adhesion and show cells in their activated state (spherical with extended filopodia) forming aggregates for all processing methods (Figure 5B). Quantification of platelet adhesion shows that platelets tend to adhere more to

the decellularized scaffolds (SDS and EtAc treated) compared to glutaraldehyde stabilized grafts. However, no significant difference was observed between the decellularization treatments nor between either EtAc or SDS and the glutaraldehyde grafts (At 1 min: EtAc $0.47\pm 0.54\%$, SDS $0.87\pm 0.82\%$, Glu $0.42\pm 0.48\%$; $P>.05$. At 5 min: EtAc $2.78\pm 1.20\%$, SDS $2.99\pm 0.80\%$, Glu $1.64\pm 0.55\%$; $P>.05$) (Figure 6A). Quantification of platelet aggregates showed a significantly higher density of discrete aggregates forming on SDS compared to Glu scaffolds (At 1 min: 38.0 ± 8.5 vs. 6.6 ± 1.5 ; $P=.006$. At 5 min: 40.0 ± 4.3 vs. 17.0 ± 3.5 ; $P=.043$) (Figure 6B). Similarly, the number of aggregates formed after 1 minute of perfusion was significantly higher for SDS than EtAc (38.0 ± 8.5 vs. 12.3 ± 4.7 ; $P=.022$), and an analogous trend was observed at 5 minutes with no significant difference (24.8 ± 21.8 vs. 40.0 ± 11.4 ; $P>.05$). When comparing the seven discrete experiments at 1 and 5 minutes, no clear correlation was observed between the number of aggregates and total platelet coverage for SDS and Glu (At 1 min: $R^2=0.4249$ and $R^2=0.5043$; at 5 min: $R^2=0.1710$ and $R^2=0.0881$ respectively) (Supplementary data 1). Conversely, EtAc decellularization resulted in increased variability in the number of aggregates formed, but was highly correlated with total platelet coverage ($R^2=0.89$ at 1 min and $R^2=0.91$ at 5 min). Overall, for a given percent platelet coverage, a higher density of discrete aggregates was observed on SDS compared to Glu and EtAc treated scaffolds (Figure 6C). Analysis of the average surface area covered per platelet shows larger development of the EtAc and Glu aggregates when compared to SDS aggregates (EtAc 0.102 ± 0.013 , Glu 0.043 ± 0.006 vs. SDS 0.074 ± 0.009 ; $P=.018$ and $P=.045$ respectively) (Figure 6D).

DISCUSSION

The aim of these investigations was to determine the effects of commonly used chemical processing treatments on *ex-vivo* derived scaffolds in order to generate an optimized biocompatible support for vascular tissue regeneration. The response of the graft to different processing treatments was analyzed to define the effects on scaffold architecture, mechanics, and peripheral cell adhesion. Two decellularization methods were evaluated and compared to traditional glutaraldehyde crosslinking that has been used clinically for over 35 years[4, 36].

The process of decellularizing *ex vivo*-derived materials can result in significant changes in the vessels ECM and gross architecture. These changes can negatively affect cell adhesion as binding sites are modified as well as tissue mechanics that, if adverse, have been shown to be predictive of graft failure. Tensile analysis over the arterial pressure range (80 to 120 mmHg) demonstrated glutaraldehyde treatment to display increased stiffness and decreased strain. These observations can be linked to the alterations in grafts structure as glutaraldehyde treated samples showed fusion of ECM fibers to form continuous smooth surfaces. By contrast, the more fibrous structure of the decellularized vessels displayed a decrease in material stiffness and an increase in strain values. Relative to native vessels, the decellularized scaffolds were more elastic; however, in the context of tissue engineering previous investigations have shown that reseeded HUVs displayed an increase in stiffness more indicative of native vessels after construct remodeling[12, 14].

In order to assess both short and long-term immune acceptance of grafting materials, it is key to understand how processing treatments influence scaffold thrombogenicity and immunogenicity. Early failure of current small diameter bypass vessels is largely attributed to thrombotic events that are initiated by an activated or absent endothelium. We have previously shown the ability of endothelial cells to adhere to the lumen of the processed HUV[15]; however, endothelial cells are often damaged during surgery or lost during reperfusion making the thrombogenicity of the acellular material a critical issue. Thus, these investigations assessed platelet interactions with the luminal surface when exposed to physiologically relevant hemodynamic conditions. A modified parallel plate flow chamber that allows observation of cell adhesion to opaque materials provided a unique platform to assess material-cell interactions[33]. Results show an increasing trend of adhesion to the decellularized materials compared to glutaraldehyde treated scaffolds. Analyses of the platelet adhesion and aggregation pattern suggested more sites where available for initial platelet attachment to SDS treated grafts, however aggregates were typically larger on Glu treated grafts. This supports clinical observations that glutaraldehyde crosslinking reduces platelet adhesion on allografts, but the surface retains a degree of biological activity[36]. It also suggests the mechanism of thrombus formation in glutaraldehyde stabilized grafts is driven by development of a few initial aggregates. By comparison, adhesion sites on SDS decellularized vessels appear to be more readily accessible as noted by a disrupted basement membrane exposing the underlying ECM. Similarly, comparison of the two decellularization treatments show a less aggressive initial adhesion of platelets to EtAc than SDS grafts and development of larger aggregates on EtAc, with a high correlation between the adhesion and aggregation processes. The observed reduction in instantaneous adhesion and the parallelism in the adhesion/aggregation pattern to treatments currently used in the clinic (Glu) suggests EtAc treatments may be a more suitable processing treatment than SDS when aiming to minimize graft thrombogenicity while preserving remodeling capacities.

While most immunogenicity testing has been based on observing lymphocyte and monocyte recruitment, studies have shown that neutrophils play an important role during xenograft and allograft rejection[37–40]. Previous observations have also shown extracts derived from decellularized pulmonary vessels to have a decrease in lymphocyte and monocyte recruitment compared to native vessels, but no reduction in neutrophils[40]. In line with these previous works, our investigations aimed to further analyze neutrophil behavior when in contact with differentially processed human umbilical veins. Interestingly, increased neutrophil adhesion was found on decellularized rather than crosslinked vessels. Little is currently understood of this phenomenon, as neutrophils are not known to specifically adhere to a denuded basement membrane. A possible explanation has been given by Bastian et al.[41] who demonstrated that specific ECM proteins from the native tissue that usually inhibit granulocyte adhesion may be removed by decellularization processes. Importantly, neutrophil recruitment does not necessarily imply graft rejection as neutrophils are also involved in tissue remodeling. They initiate the reparative and remodeling process via recruitment of monocytes that have the capacity to differentiate into the “healer” M2 macrophage phenotype[42]. Research continues toward the characterization of monocytes recruitment and differentiation processes as a tool to positively control inflammatory responses and promote positive tissue remodeling[43].

By understanding the impact of tissue processing on cell adhesion, processing treatments can be optimized to not only reduce thrombogenicity and immunogenicity but also to favor recellularization. The creation of a functional endothelium and vascular wall are crucial for the development of a graft with improved patency rates. Previous studies have shown that endothelial cells have a higher adhesion efficiency on the EtAc than SDS processed HUV[15], and that EtAc grafts support increased oxygen diffusion, muscle cell proliferation and migration compared to scaffolds treated with SDS[44]. These results suggest EtAc treatment is preferential to SDS to generate an acellular scaffold with enhanced remodeling features.

CONCLUSIONS

These findings have shown chemical treatments used to reduce the broader immunogenicity of these model *ex vivo*-derived vascular grafts influence mechanical properties and surface chemistries. Chemical effects alter the material's elastic properties and peripheral cell adhesion both of which are shown to be determinants of graft patency. From the treatments assessed we have determined that EtAc may be preferential to SDS as a decellularization approach when developing acellular scaffolds for vascular regeneration.

Supplementary Material

Refer to Web version on PubMed Central for supplementary material.

ACKNOWLEDGEMENTS

The authors would like to thank Dr. Christopher Cogle and the UF Clinical and Translational Science Institute for their assistance with blood draws. We also thank Dr. Cogle for contributing the GFP+ HL-60 cells for this study and Jorge Sefair for his comments on the statistical analyses.

SOURCES OF FUNDING

This work was supported by the National Institutes of Health (R01-HL088207 and R01-HL088207-03S1).

REFERENCES

1. Garrett HE, Dennis EW, DeBakey ME. Aortocoronary bypass with saphenous vein graft. Seven-year follow-up. JAMA. 1973; 223:792–794. [PubMed: 4567689]
2. Gibson KD, Gillen DL, Caps MT, Kohler TR, Sherrard DJ, Stehman-Breen CO. Vascular access survival and incidence of revisions: A comparison of prosthetic grafts, simple autogenous fistulas, and venous transposition fistulas from the United States Renal Data System Dialysis Morbidity and Mortality Study. Journal of Vascular Surgery. 2001; 34:694–700. [PubMed: 11668326]
3. Johnson WC, Lee KK. A comparative evaluation of polytetrafluoroethylene, umbilical vein, and saphenous vein bypass grafts for femoral-popliteal above-knee revascularization: a prospective randomized Department of Veterans Affairs cooperative study. J. Vasc. Surg. 2000; 32:268–277. [PubMed: 10917986]
4. Dardik H, Wengerter K, Qin F, Pangilinan A, Silvestri F, Wolodiger F, et al. Comparative decades of experience with glutaraldehyde-tanned human umbilical cord vein graft for lower limb revascularization: An analysis of 1275 cases. Journal of Vascular Surgery. 2002; 35:64–71. [PubMed: 11802134]
5. Dardik, A.; Dardik, H. Umbilical Vein Grafts for Lower Limb Revascularization. In: Bhattacharya, N.; Stubblefield, P., editors. Regenerative Medicine Using Pregnancy-Specific Biological

Substances [Internet]. Springer London: 2011. p. 189-198. Available from: http://link.springer.com/chapter/10.1007/978-1-84882-718-9_19 [cited 2014 Oct 20]

6. Migneault I, Dartiguenave C, Bertrand MJ, Waldron KC. Glutaraldehyde: behavior in aqueous solution, reaction with proteins, and application to enzyme crosslinking. *BioTechniques*. 2004; 37:790–796. 798–802. [PubMed: 15560135]
7. Simionescu A, Simionescu D, Deac R. Lysine-enhanced glutaraldehyde crosslinking of collagenous biomaterials. *J. Biomed. Mater. Res*. 1991; 25:1495–1505. [PubMed: 1794997]
8. Eybl E, Grimm M, Grabenwöger M, Böck P, Müller MM, Wolner E. Endothelial cell lining of bioprosthetic heart valve materials. *J. Thorac. Cardiovasc. Surg*. 1992; 104:763–769. [PubMed: 1355151]
9. Gough JE, Scotchford CA, Downes S. Cytotoxicity of glutaraldehyde crosslinked collagen/poly(vinyl alcohol) films is by the mechanism of apoptosis. *J. Biomed. Mater. Res*. 2002; 61:121–130. [PubMed: 12001254]
10. Pektok E, Nottelet B, Tille J-C, Gurny R, Kalangos A, Moeller M, et al. Degradation and Healing Characteristics of Small-Diameter Poly(ϵ -Caprolactone) Vascular Grafts in the Rat Systemic Arterial. *Circulation*. 2008; 118:2563–2570. [PubMed: 19029464]
11. Nemcova S, Noel AA, Jost CJ, Gloviczki P, Miller VM, Brockbank KG. Evaluation of a xenogeneic acellular collagen matrix as a small-diameter vascular graft in dogs--preliminary observations. *J Invest Surg*. 2001; 14:321–330. [PubMed: 11905500]
12. Daniel J, Abe K, McFetridge PS. Development of the human umbilical vein scaffold for cardiovascular tissue engineering applications. *ASAIO J*. 2005; 51:252–261. [PubMed: 15968956]
13. Gui L, Muto A, Chan SA, Breuer CK, Niklason LE. Development of decellularized human umbilical arteries as small-diameter vascular grafts. *Tissue Eng Part A*. 2009; 15:2665–2676. [PubMed: 19207043]
14. Tosun Z, McFetridge PS. Improved recellularization of ex vivo vascular scaffolds using directed transport gradients to modulate ECM remodeling. *Biotechnol. Bioeng*. 2013; 110:2035–2045. [PubMed: 23613430]
15. Uzarski JS, Van De Walle AB, McFetridge PS. Preimplantation processing of ex vivo-derived vascular biomaterials: effects on peripheral cell adhesion. *J Biomed Mater Res A*. 2013; 101:123–131. [PubMed: 22825780]
16. Kasimir M-T, Rieder E, Seebacher G, Nigisch A, Dekan B, Wolner E, et al. Decellularization does not eliminate thrombogenicity and inflammatory stimulation in tissue-engineered porcine heart valves. *J. Heart Valve Dis*. 2006; 15:278–286. discussion 286. [PubMed: 16607912]
17. Hashi CK, Derugin N, Janairo RRR, Lee R, Schultz D, Lotz J, et al. Antithrombogenic modification of small-diameter microfibrillar vascular grafts. *Arterioscler. Thromb. Vasc. Biol*. 2010; 30:1621–1627. [PubMed: 20466974]
18. Lin PJ, Chang CH, Lee YS, Chou YY, Chu JJ, Chang JP, et al. Acute endothelial reperfusion injury after coronary artery bypass grafting. *Ann. Thorac. Surg*. 1994; 58:782–788. [PubMed: 7944703]
19. Sasaki Y, Suehiro S, Becker A, Kinoshita H, Ueda M. Role of endothelial cell denudation and smooth muscle cell dedifferentiation in neointimal formation of human vein grafts after coronary artery bypass grafting: therapeutic implications. *Heart*. 2000; 83:69–75. [PubMed: 10618339]
20. Libby P, Pober JS. Chronic rejection. *Immunity*. 2001; 14:387–397. [PubMed: 11336684]
21. Mäyränpää M, Simpanen J, Hess MW, Werkkala K, Kovanen PT. Arterial endothelial denudation by intraluminal use of papaverine-NaCl solution in coronary bypass surgery. *Eur J Cardiothorac Surg*. 2004; 25:560–566. [PubMed: 15037272]
22. Quillard T, Coupel S, Coulon F, Fitau J, Chatelais M, Cuturi MC, et al. Impaired Notch4 activity elicits endothelial cell activation and apoptosis: implication for transplant arteriosclerosis. *Arterioscler. Thromb. Vasc. Biol*. 2008; 28:2258–2265. [PubMed: 18802018]
23. Brown MA, Zhang L, Levering VW, Wu J-H, Satterwhite LL, Brian L, et al. Human umbilical cord blood-derived endothelial cells reendothelialize vein grafts and prevent thrombosis. *Arterioscler. Thromb. Vasc. Biol*. 2010; 30:2150–2155. [PubMed: 20798381]

24. Barnes CA, Brison J, Michel R, Brown BN, Castner DG, Badylak SF, et al. The surface molecular functionality of decellularized extracellular matrices. *Biomaterials*. 2011; 32:137–143. [PubMed: 21055805]
25. Gratzner PF, Harrison RD, Woods T. Matrix alteration and not residual sodium dodecyl sulfate cytotoxicity affects the cellular repopulation of a decellularized matrix. *Tissue Eng*. 2006; 12:2975–2983. [PubMed: 17518665]
26. Bhuyan AK. On the mechanism of SDS-induced protein denaturation. *Biopolymers*. 2010; 93:186–199. [PubMed: 19802818]
27. Montoya CV, McFetridge PS. Preparation of ex vivo-based biomaterials using convective flow decellularization. *Tissue Eng Part C Methods*. 2009; 15:191–200. [PubMed: 19196128]
28. Crapo PM, Gilbert TW, Badylak SF. An overview of tissue and whole organ decellularization processes. *Biomaterials*. 2011; 32:3233–3243. [PubMed: 21296410]
29. Zhang J, Bergeron AL, Yu Q, Sun C, McIntire LV, López JA, et al. Platelet aggregation and activation under complex patterns of shear stress. *Thromb. Haemost.* 2002; 88:817–821. [PubMed: 12428100]
30. Coughlin MF, Sohn DD, Schmid-Schönbein GW. Recoil and stiffening by adherent leukocytes in response to fluid shear. *Biophys. J.* 2008; 94:1046–1051. [PubMed: 17921217]
31. Balasubramanian V, Grabowski E, Bini A, Nemerson Y. Platelets, circulating tissue factor, and fibrin colocalize in ex vivo thrombi: real-time fluorescence images of thrombus formation and propagation under defined flow conditions. *Blood*. 2002; 100:2787–2792. [PubMed: 12351386]
32. Van de Walle AB, Fontenot J, Spain TG, Brunski DB, Sanchez ES, Keay JC, et al. The role of fibrinogen spacing and patch size on platelet adhesion under flow. *Acta Biomater.* 2012; 8:4080–4091. [PubMed: 22820307]
33. Uzarski JS, Van de Walle AB, McFetridge PS. In Vitro Method for Real-time, Direct Observation of Cell-Vascular Graft Interactions Under Simulated Blood Flow. *Tissue Eng Part C Methods*. 2013
34. Dardik H, Dardik II. Successful arterial substitution with modified human umbilical vein. *Ann. Surg.* 1976; 183:252–258. [PubMed: 816263]
35. Mollinedo F, López-Pérez R, Gajate C. Differential gene expression patterns coupled to commitment and acquisition of phenotypic hallmarks during neutrophil differentiation of human leukaemia HL-60 cells. *Gene*. 2008; 419:16–26. [PubMed: 18547747]
36. Neufang A, Espinola-Klein C, Dorweiler B, Messow CM, Schmiedt W, Vahl CF. Femoropopliteal prosthetic bypass with glutaraldehyde stabilized human umbilical vein (HUV). *J. Vasc. Surg.* 2007; 46:280–288. [PubMed: 17600663]
37. Cardozo LAM, Rouw DB, Ambrose LR, Midulla M, Florey O, Haskard DO, et al. The neutrophil: the unnoticed threat in xenotransplantation? *Transplantation*. 2004; 78:1721–1728. [PubMed: 15614144]
38. Buonocore S, Surquin M, Le Moine A, Abramowicz D, Flamand V, Goldman M. Amplification of T-cell responses by neutrophils: relevance to allograft immunity. *Immunol. Lett.* 2004; 94:163–166. [PubMed: 15275962]
39. Hirayama S, Shiraishi T, Shirakusa T, Higuchi T, Miller EJ. Prevention of Neutrophil Migration Ameliorates Rat Lung Allograft Rejection. *Mol Med*. 2006; 12:208–213. [PubMed: 17225868]
40. Rieder E, Nigisch A, Dekan B, Kasimir M-T, Mühlbacher F, Wolner E, et al. Granulocyte-based immune response against decellularized or glutaraldehyde cross-linked vascular tissue. *Biomaterials*. 2006; 27:5634–5642. [PubMed: 16889827]
41. Bastian F, Stelzmüller M-E, Kratochwill K, Kasimir M-T, Simon P, Weigel G. IgG deposition and activation of the classical complement pathway involvement in the activation of human granulocytes by decellularized porcine heart valve tissue. *Biomaterials*. 2008; 29:1824–1832. [PubMed: 18258297]
42. Kou PM, Babensee JE. Macrophage and dendritic cell phenotypic diversity in the context of biomaterials. *J Biomed Mater Res A*. 2011; 96:239–260. [PubMed: 21105173]
43. Hibino N, Yi T, Duncan DR, Rathore A, Dean E, Naito Y, et al. A critical role for macrophages in neovessel formation and the development of stenosis in tissue-engineered vascular grafts. *FASEB J*. 2011; 25:4253–4263. [PubMed: 21865316]

44. Moore M, Sarntinoranont M, McFetridge P. Mass transfer trends occurring in engineered ex vivo tissue scaffolds. *J Biomed Mater Res A*. 2012; 100:2194–2203. [PubMed: 22623220]

Author Manuscript

Author Manuscript

Author Manuscript

Author Manuscript

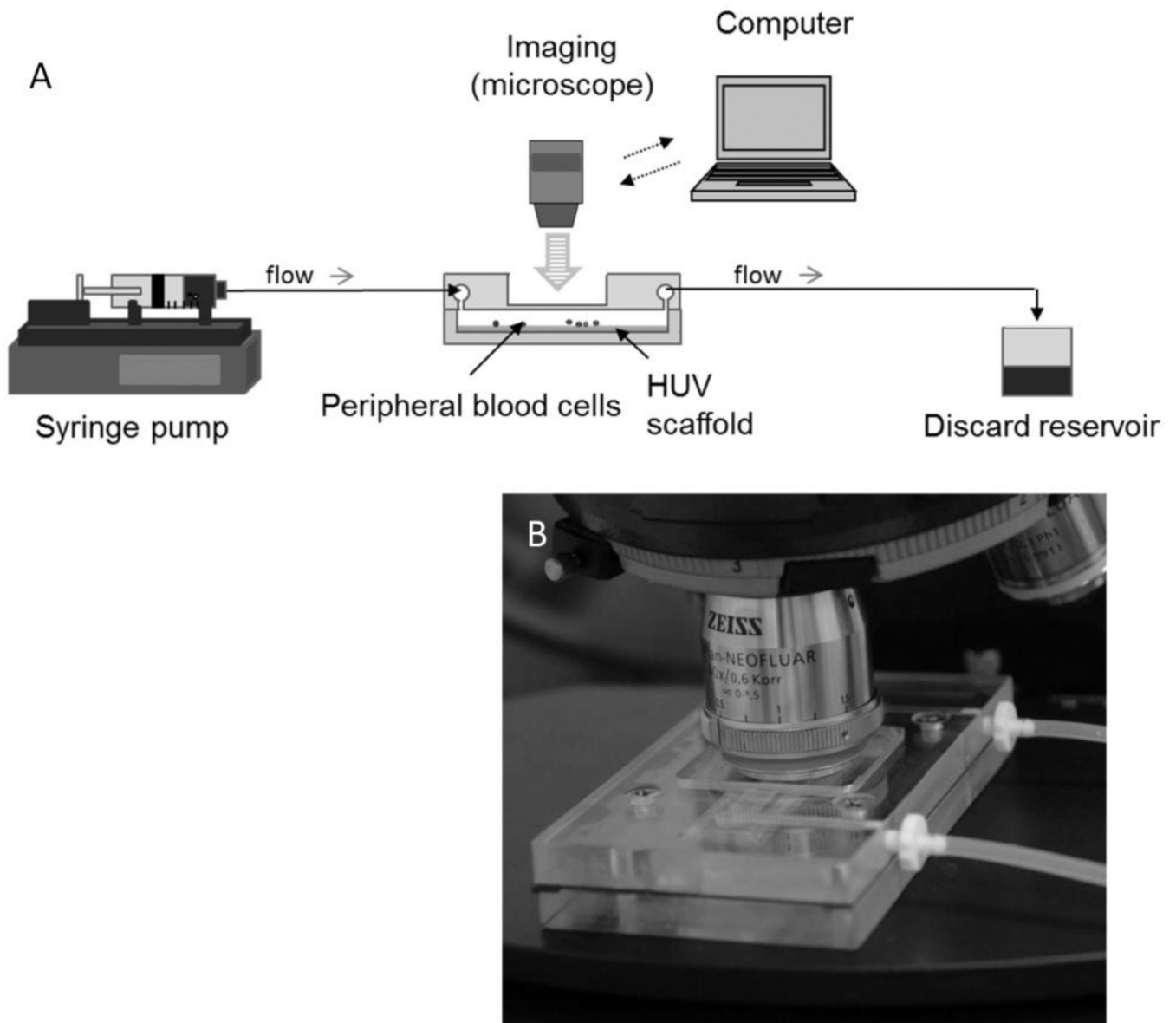


Figure 1. Perfusion design

A newly designed flow chamber is used to observe platelet and leukocyte adhesion to the graft materials in real-time. Shear conditions are controlled by modulating the bulk flow rate using a high capacity syringe pump. Images are recorded via a high resolution Zeiss Axiocam monochrome Rev 3 digital camera. (A) Schematic of the perfusion circuit. (B) Photograph of the newly designed flow chamber.

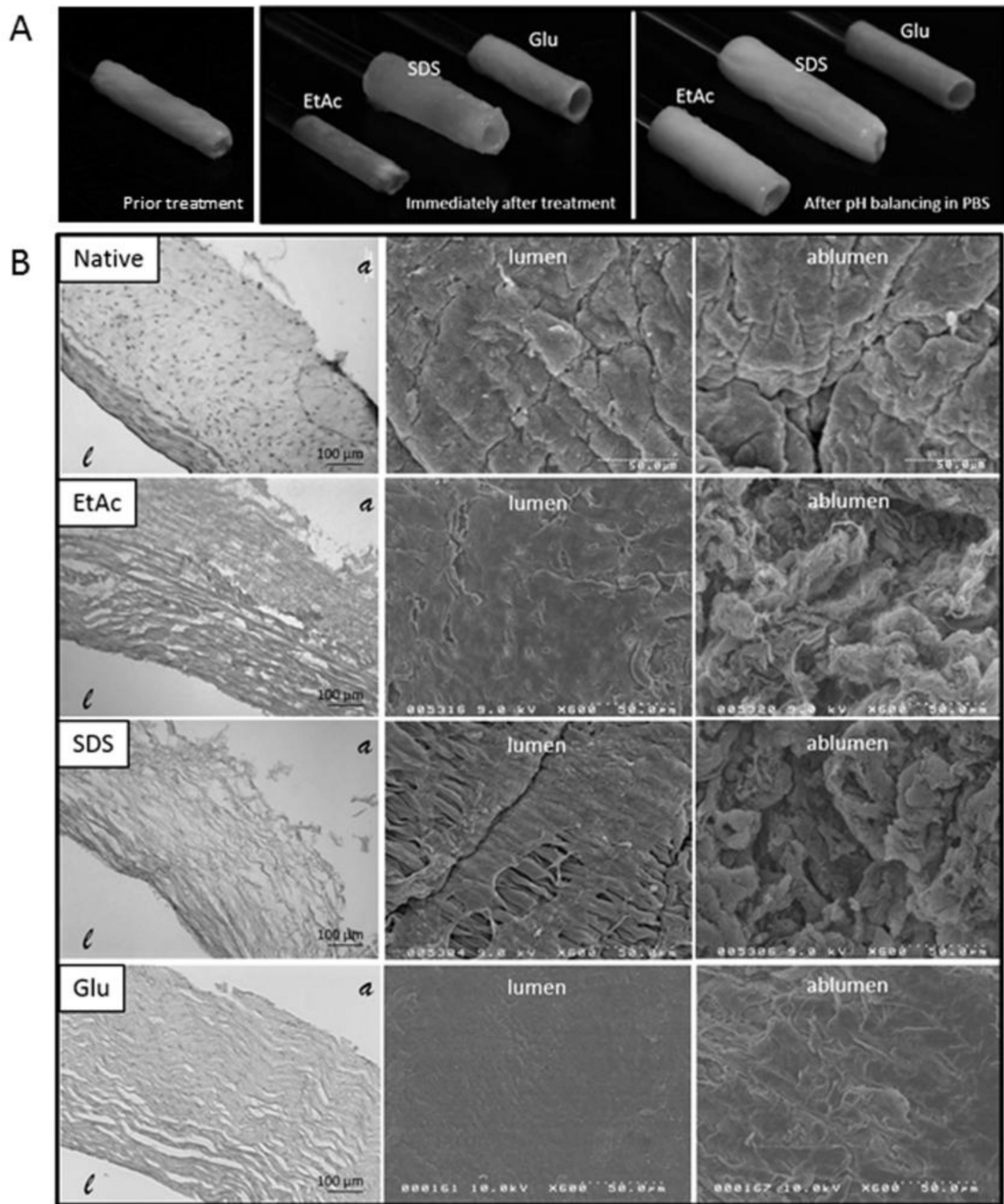


Figure 2. Processing influence on the scaffold architecture

Extracted Human Umbilical Veins (HUV) were either decellularized with one of two different chemical treatments or cross-linked with glutaraldehyde. Shown in the top row (A) are representative images of HUV scaffolds immediately following treatment and after subsequent rinsing in PBS. The micro-architecture of the processed scaffolds is shown in (B), first by H&E staining (left), then by SEM imaging of the luminal (middle), and abluminal (right) surface. Treatments are labeled as follows: (EtAc) Ethanol/Acetone

decellularization, (SDS) Sodium Dodecyl Sulfate decellularization, and (Glu) Glutaraldehyde crosslinking. represents the lumen of the HUV and the ablumen.

Author Manuscript

Author Manuscript

Author Manuscript

Author Manuscript

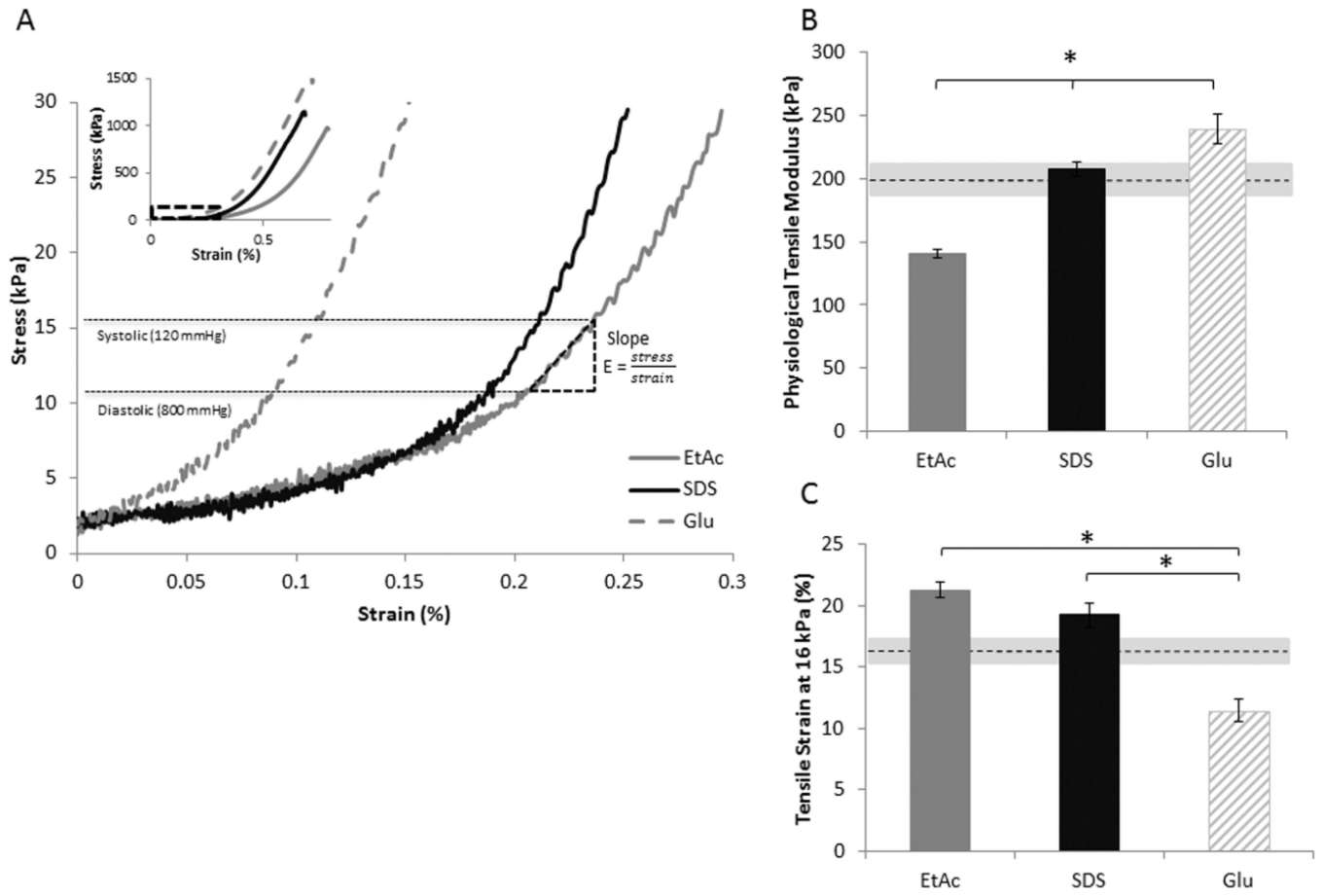


Figure 3. Scaffold mechanical properties

The mechanics of the HUV were tested after processing treatments followed by subsequent rinsing/sterilization. Graphs show (A) representative strain/stress curves, inset showing the complete profile with an enlargement over the physiological range, B) tensile modulus in the physiological range (from 11 to 16 kPa, represented by E in (A)), and C) tensile strain at 16 kPa. (n=3, * P<.05) Dashed lines represent the scaffold prior to chemical processing, and the grey areas surrounding the dash lines indicate the standard error.

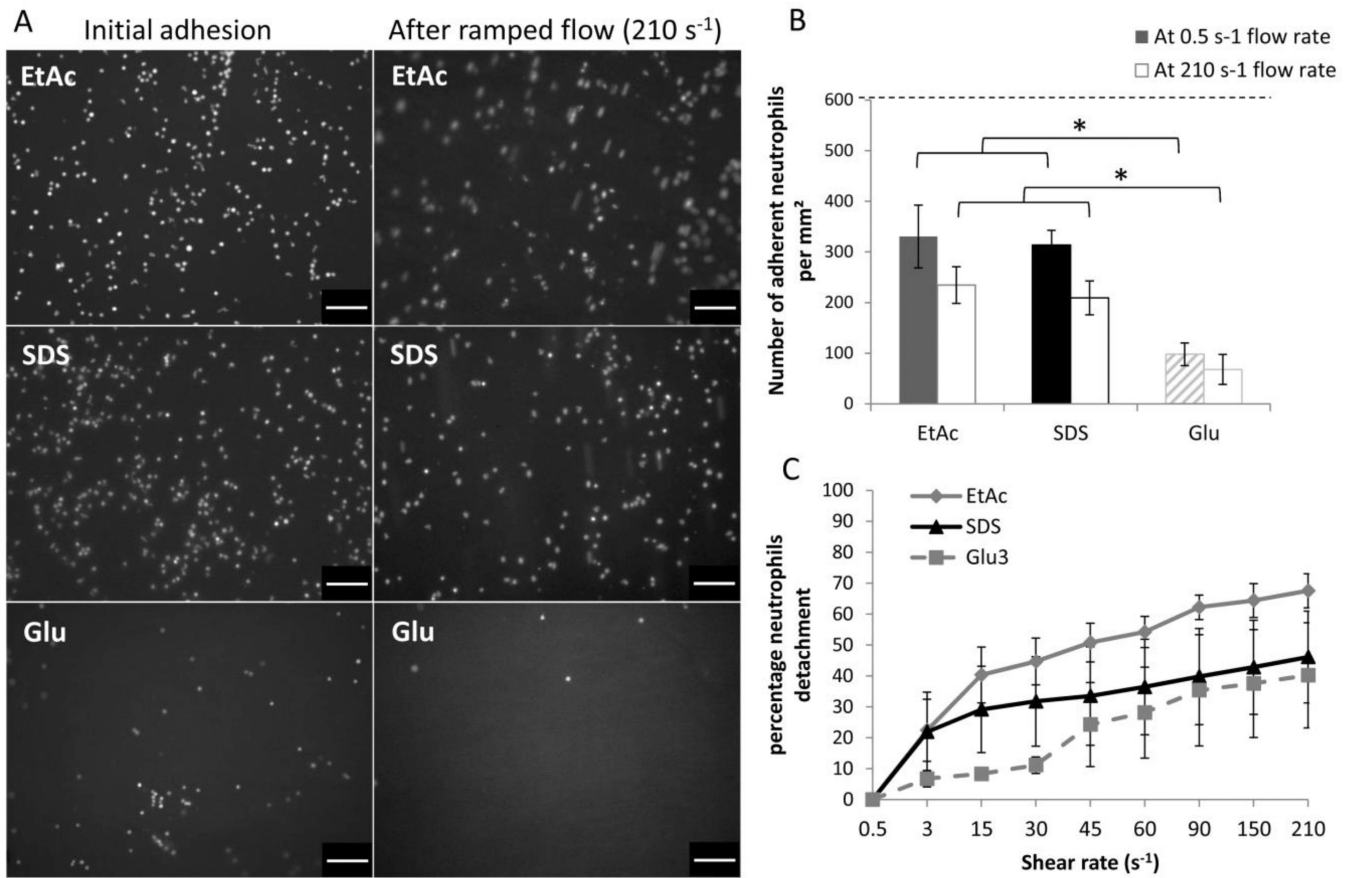


Figure 4. Neutrophil adhesion to processed HUV

HL-60 differentiated as neutrophils were incubated with HUV for 5 hours. After incubation and subsequent exposure to a 210 s⁻¹ flow, the neutrophils adhering to the luminal surface of the vein were (A) observed (scale bar: 100 μm) and (B) quantified (* P<.05, the dashed line represents the amount of neutrophils incubated). Neutrophil detachment as a function of shear was also observed (C). After incubation, a ramping flow was applied and the percentage of neutrophils detaching was quantified for each shear condition. (n=4).

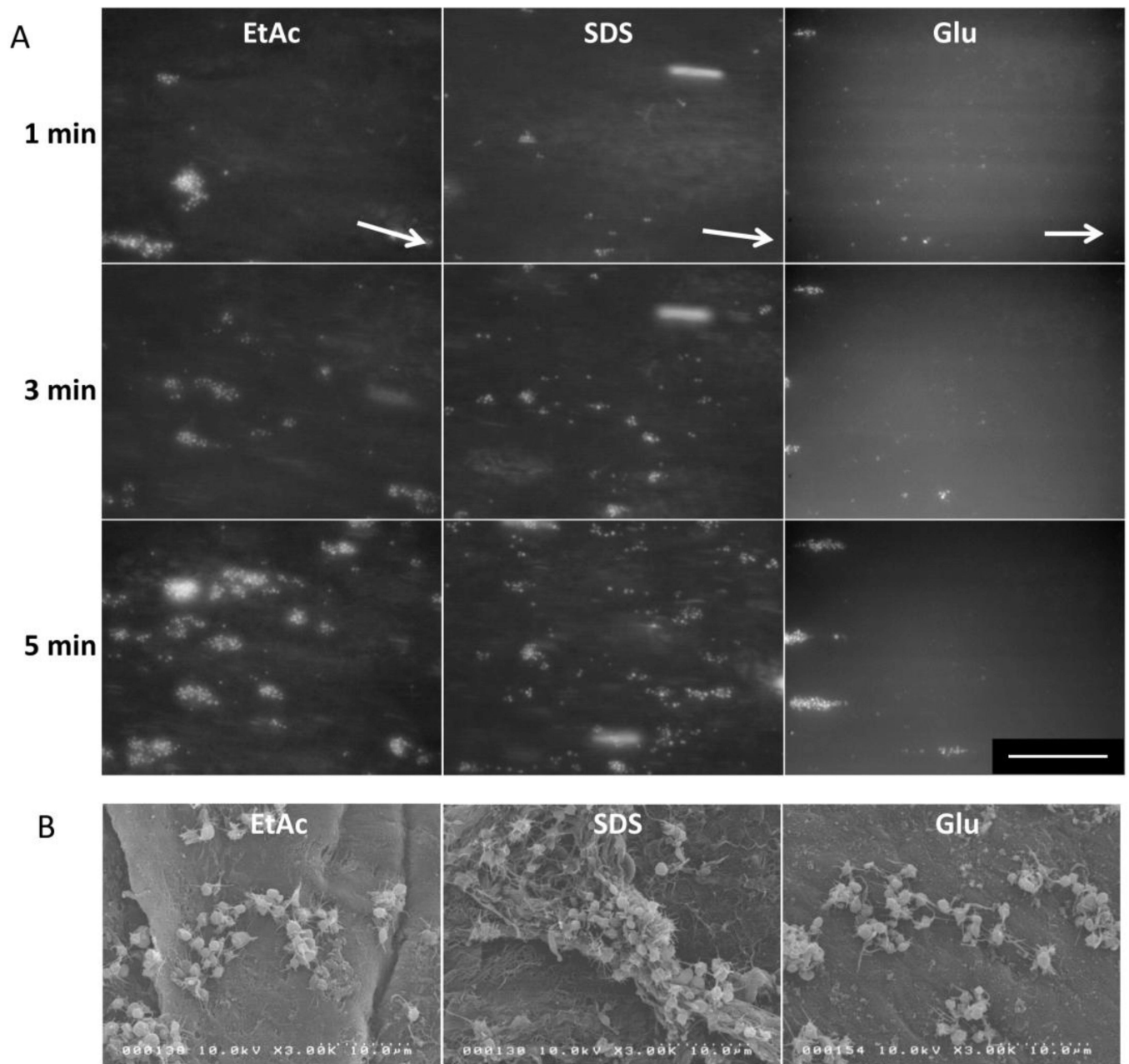


Figure 5. Qualitative visual assessment of platelet adhesion and aggregates formation

A) Representative fluorescent images of platelet adhesion to the lumen of processed HUV over time, under a shear rate of 210 s^{-1} . White arrows represent flow direction. Scale bar: $100 \mu\text{m}$. B) After five minutes of whole blood perfusion at a shear rate of 210 s^{-1} , platelet aggregates were imaged using scanning electron microscopy.

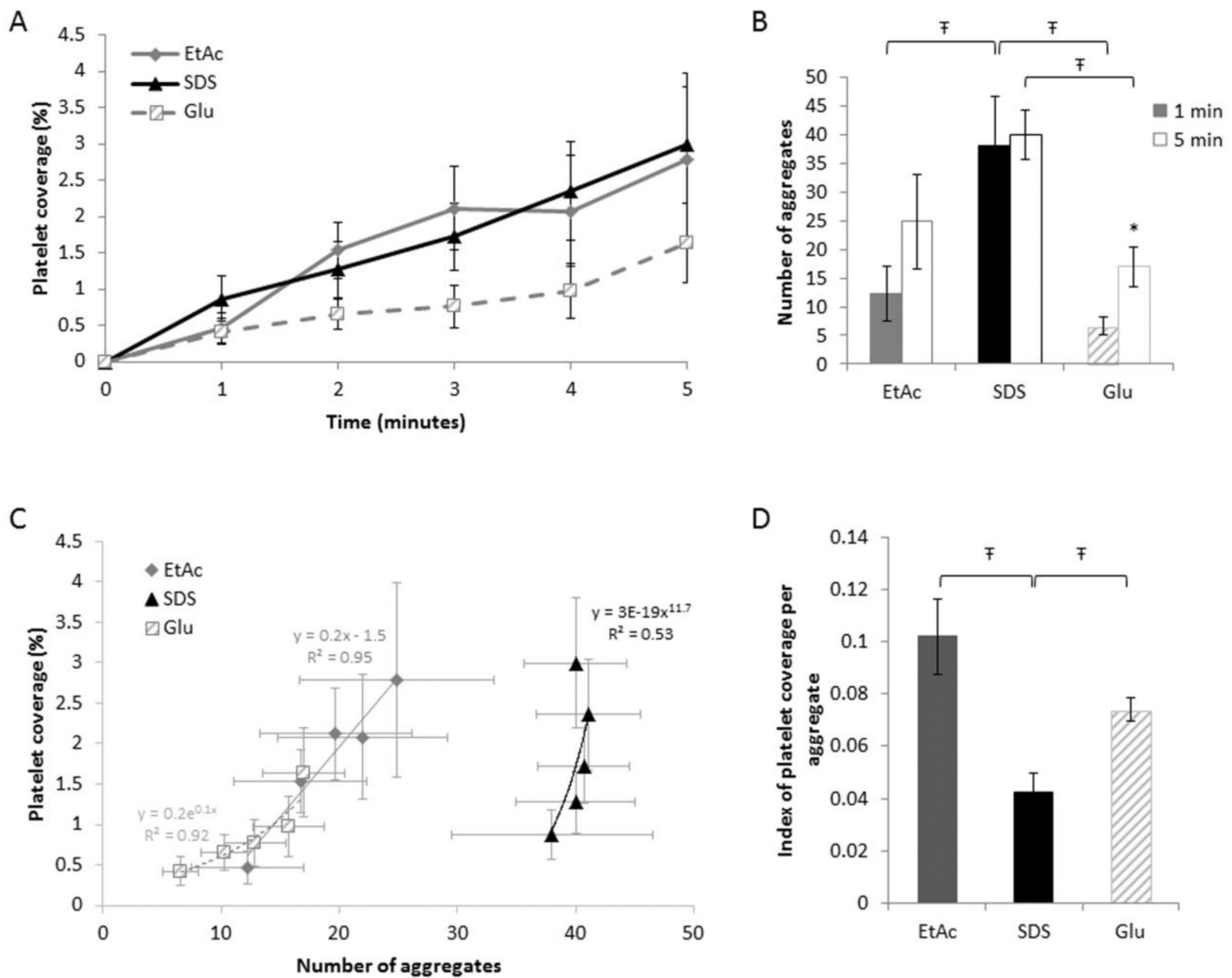


Figure 6. Progression of platelet adhesion and aggregation

A) Real-time analysis of the total platelet accumulation on the lumen of the HUV at a given shear rate of 210 s^{-1} . Each data point represents the mean \pm S.E. for 7 separate experiments. B) After one and five minutes of perfusion, the number of platelet aggregates was quantified ($\text{F P} < .05$ between the three treatments, * $\text{P} < .05$ between 1 and 5 minutes for each treatment). C) Correlation between platelet aggregation and surface coverage was assessed at 1, 2, 3, 4, and 5 minutes. Each data point represents the mean platelet aggregates correlated to the corresponding total area covered with platelets for seven separate experiments. D) An index indicating the overall surface area covered by one platelet was calculated for each treatment ($\text{F P} < .05$ between the three treatments).